



Integration of satellite remote sensing and geophysical techniques (electrical resistivity tomography and ground penetrating radar) for landslide characterization at Kunjethi (Kalimath), Garhwal Himalaya, India

Suresh Kannaujiya¹ · Shovan Lal Chatteraj¹ · Dilhani Jayalath² · Prashant Kumar Champati ray¹ · Kushank Bajaj¹ · Shilpika Podali¹ · M. P. S. Bisht³

Received: 29 July 2016 / Accepted: 27 July 2019 / Published online: 3 August 2019
© Springer Nature B.V. 2019

Abstract

During the extreme precipitation event of 15th–17th June 2013 in Garhwal Himalaya, glacial lake outburst flooding accompanied by numerous landslides and flash flood events caused widespread death and destruction. Many hill slopes and steep river banks had developed fractures and fissures indicative of landslides and one such scarp was observed at Kunjethi (Kalimath) village on satellite images during routine analysis. Rainfall threshold analysis for years 2012, 2013, 2014 and 2015 has confirmed that it was the main triggering factor which happened due to extreme precipitation in June 2013 leading to scarp development and initiation of landslide. In order to characterize the landslide and get subsurface information, two highly cost-effective and fast non-invasive geophysical techniques, electrical resistivity tomography (ERT) and ground penetrating radar (GPR), were used. Four ERT profiles and one GPR radargram profile were used to determine the approximate depth to slip surface, which is inferred around 15–19 m. Integration of satellite remote sensing, geophysical studies and field observations have been used to demarcate the maximum possible slide zone. This study reiterates that earth observation tools in integration with faster, non-invasive and cost-effective geophysical techniques can establish the slip surface, which is an essential information required for landslide hazard mitigation measures.

Keywords ERT · GPR · Landslide · Slip surface · Himalaya · Rainfall threshold · Satellite image · Risk management

✉ Suresh Kannaujiya
skannaujiya@iirs.gov.in

¹ Indian Institute of Remote Sensing, Dehradun, India

² National Building Research Organization, Kalutara, Sri Lanka

³ Uttarakhand Space Application Centre, Dehradun, Uttarakhand, India

1 Introduction

As it is well known, the mighty Himalaya was formed by the process of continent–continent collision. At the same time, it has emerged as one of the global hot spot of mass wasting process such as landslides and snow avalanches mainly due to active tectonism, extreme precipitation events associated with heavy south-west monsoon and climate change (Petley 2012). In the recent past, the most devastating and catastrophic event occurred between 15th and 17th June 2013 due to extreme precipitation resulting in glacial lake outburst flood (GLOF). This event subsequently resulted in widespread landslides and flash floods that affected almost entire Garhwal Himalaya covering five districts of Uttarakhand state in north India (Champati ray et al. 2013; Dobhal et al. 2013). During this event, numerous landslides occurred leading to development of ground subsidence, at places. Preliminary survey revealed a hill ward large scarp and a near-river active landslide on satellite image near Kalimath. Kalimath is located at about 20 km from Kedarnath, which also witnessed the effect of 2013 Kedarnath event. The scarp and active landslide developed in parts of an old large landslide zone posed danger for damaging access road, human settlement and even a possibility of river blockade in the event of a large landslide. Therefore, an immediate need was felt to characterize landslide and obtain crucial geotechnical information that would help to avert potential damage due to landslide.

A landslide is a complex geologic body composed of a combination of layers having contrasting and gradational physical properties and are caused by a host of geological, geotechnical and climatic factors (Bogoslovsky and Ogilvy 1977; Cruden 1991). A multidisciplinary approach, based on geological, geomorphological and geophysical observations aided by geodetic studies, meteorological data analysis and satellite observations, is often recommended to understand the complex phenomenon of a landslide in a holistic way (Perrone et al. 2006; Castellanos Abella and Van Westen 2008). In order to assess the temporal and spatial probability of occurrence and magnitude of the landslide, it is important to identify the failure plane/slip surface. This work has also shown the beauty of using remote sensing data which caters to an immediate, cost-effective way to get information about the landslide. However, the remote sensing-based outputs required subsequent geological and geomorphological data validated by shallow surface geophysical investigations.

Albeit, cost of drilling, conventional geotechnical investigations remained as mainstay in slope characterization (Hunt 1984). Moreover, the engineering geological processes mostly deal with geo-mechanical properties of the rocks/soil, not the physical properties of them, *sensu stricto*. But it is time and again felt that the mechanical and physical properties both complement each other, to the extent possible for better characterization subsurface. Therefore, attempts have been made to explore geophysical methods that can provide subsurface information at a reasonable cost at least in the initial stages of investigation. Hence, it can be considered as a complementary alternative to costly drilling exercises, wherever applicable (McGuffey et al. 1996; Hack 2000; Friedel et al. 2006; Jongmans and Garambois 2007; Sass et al. 2008).

One of the most used methods for subsurface characterization is the electrical resistivity tomography (ERT) techniques, which has been applied to study the electrical properties of subsurface and to identify the failure plane/slip surface of the landslide, which is the most fundamental and important requirement of the landslide investigation (Bichler et al. 2004; Lapenna et al. 2005; Meric et al. 2005; Godio et al. 2006). GPR

(ground penetrating radar) is also used to provide detailed information about subsurface heterogeneities of the near surface. The combination of high-resolution GPR and ERT thus proved effective with varied acquisition parameters.

The primary aim of the present study is to confirm the presence of landslide scarp, its dimension as observed on satellite images and to determine depth and geometry of the slip surface of the slowly moving landslide using 2-D ERT and GPR. In addition to geophysical techniques, this study is also aimed at evaluating a relationship between rainfall trigger and landslide. This study presents a case study where different methods and data at appropriate scales have been used to characterize the landslide. Crucial inputs are received from precipitation and remote sensing data complemented by ground-based geophysical cues. A geotechnical problem in this work has been analysed in the light of geophysical, remote sensing and other ancillary sources, which expose the causative and triggering factors for landslide.

2 Study area

The study area lies in the Kaliganga river valley (that is parallel upper Mandakini river valley) close to Kalimath. It is bounded by latitude 30.564°N–30.545°N and longitude 79.074°E–79.101°E (Fig. 1). It is situated in Rudraprayag district of Uttarakhand state and covers an area of 5.64 km². The developed scarp is approximately 685 m long located above the Kunjethi-Kotma road, less than a km from the Kunjethi temple towards Guptkashi. The aerial distance from Kaliganga river to top of the scarp is approximately 500 m. The scarp extends above Kunjethi village, which is a home to about 35 families out of which 10 families (60 people) stay even during the perilous monsoon season. The scarp has been developed towards up slope of a previously formed landslide along the Kunjethi-Kotma road. The area experiences subtropical temperate climate and precipitation of 1200–1500 mm per annum (Bhattacharjee et al. 2017; Indian Meteorological Organisation, Champati ray et al. 2015; Chatteraj and Champati ray 2015; Chatteraj et al. 2017; Dohal et al. 2013). Most of the precipitation occurs during south-western summer monsoon months starting from late June to September. Rugged conical peaks dominate the region with moderate to steep slopes and elevation varies from 1250 to 1450 m. The combination of steep slopes and high precipitation during monsoon months triggers majority of the landslides in this area.

3 Geology and tectonics of the area

The study area belongs to Central Crystalline Zone of Himalaya (Valdiya et al. 1999) consisting mainly of metamorphic rocks and granitic intrusions (Fig. 2). It is divided into two major lithotectonic units namely Munsiri Group and Vaikrita Group separated by Vaikrita Thrust (Main Central Thrust—MCT-II). The former is made up of cataclastic/mylonitized rocks and granites of Middle Proterozoic, while the latter consist of medium- to high-grade metamorphic rocks and porphyritic granite gneiss (Valdiya et al. 1999). The Central Crystalline Zone is bounded by Trans-Himadri Fault in the north and Musiri Thrust (MCT-I) in the south. The area under investigation comes under Vaikrita Group consisting of gneissic and schistose rocks, a medium- to high-grade metamorphosed originally arenaceous siliciclastics, argillaceous rocks and impure carbonates, with subordinate

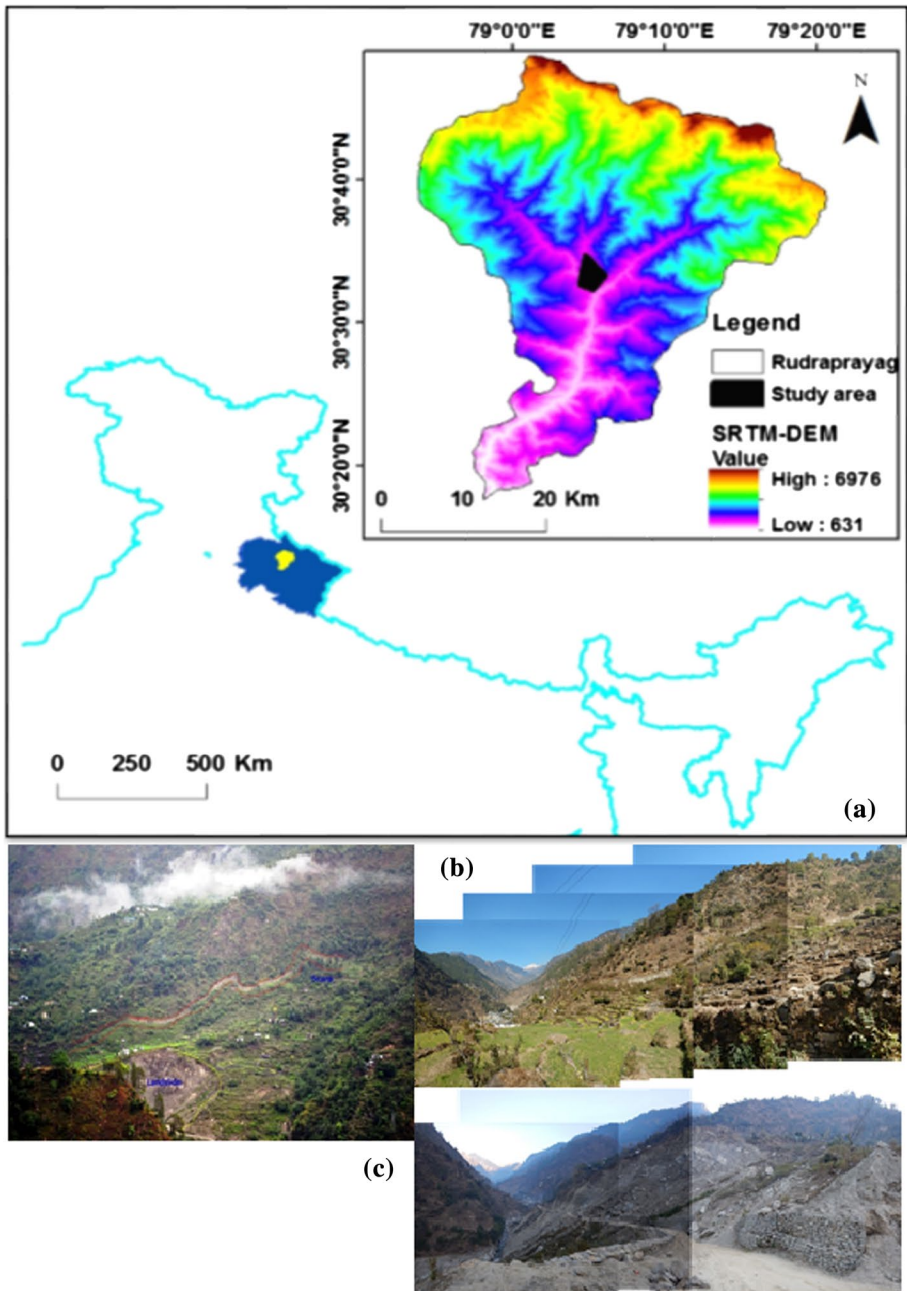


Fig. 1 **a** Study area around Kunjethi (Kalimath) village, Uttarakhand, India, **b** Panoramic view of former landslide and developed scarp and **c** developed scarp and active landslide at Kunjethi Village, Kalimath

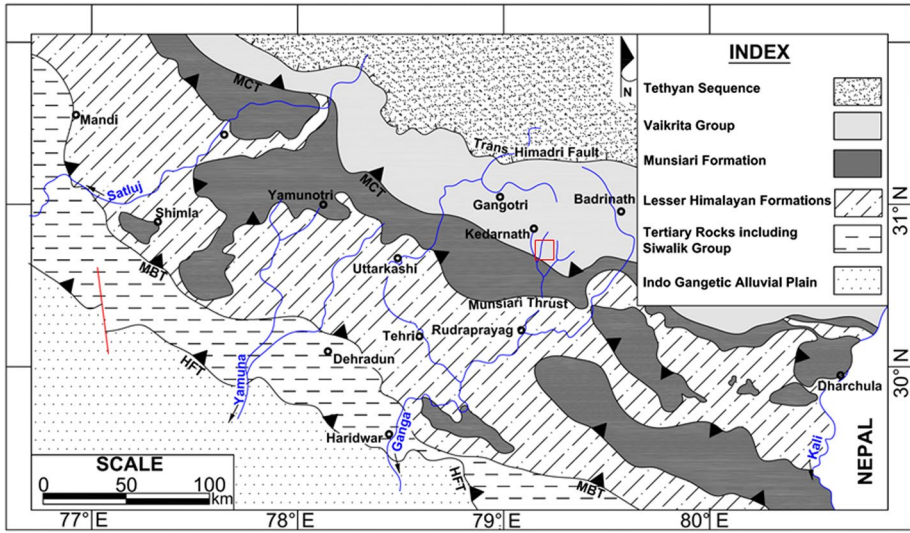


Fig. 2 Lithotectonic subdivisions of part of Western Himalayan. The rectangular box (in red) represents the study area. *MBT* Main Boundary Thrust, *HFT* Himalayan Frontal Thrust, *MCT* Main Central Thrust (symbology is as per conventional geological notations)

disseminated volcanics. The Vaikrita Group is further divided into three formations, viz. Joshimath, Pandukeshwar and Pindari (Table 1). The rocks exposed in the study area mainly belong to Joshimath Formation consisting mainly of garnetiferous schist, mica schist, marble, porphyritic biotite gneiss, sillimanite gneiss, graphitic schist (Bist and Sinha 1980). Overall, the study area is close to major discontinuities like MCT-II and represents a tectonically disturbed zone.

Geomorphologically, study area is covered mostly by high to moderately dissected hills, moderately sinus second-order rivers. The active slide portion is highly rugged, at places. The maximum height of the slided portion is around 1560 m, and rivers flows at around 1200 m MSL. Slide is covered by weathered derivatives of the rocks described above and sparse vegetation. The vulnerable slope broadly dips towards west. Sympathetic cracks parallel to arcuate source region of landslides are visible on the ground. The cracks are mostly unfilled and terminated at bedrocks laterally. Overall slope of the topography is 25° (landslide portion) to 40° (hill side). Hydrogeologically, the area falls under a discharge zone bounded by spring-fed water shoots on both the sides of landslide. The water is used by local villagers for drinking purpose also. The scarp extends from Kunjethi village and culminates at a major lineament present on the southern side of it (Fig. 3).

4 Methodology and data processing

4.1 Precipitation data analysis

Rainfall is the most common triggering factor for development of landslides during monsoon periods in the Himalayan region (Bhattacharjee et al. 2017; Champati ray et al. 2015;

Table 1 Technical details of satellite sensor used for Kunjethi landslide investigation

S. No.	Satellite/sensor	Swath	Radiometric resolution	Spatial resolution	Altitude (km)	Orbit
1	LISS-IV	23 km (max mode) 70 km (mono mode)	8 bits	5.8 at nadir	817	Sun synchronous
2	Digital Globe Quick bird	16.8 km at nadir	11 bits per pixel	61 cm PAN at nadir/ 2.44 m MSS at nadir	450	Sun synchronous

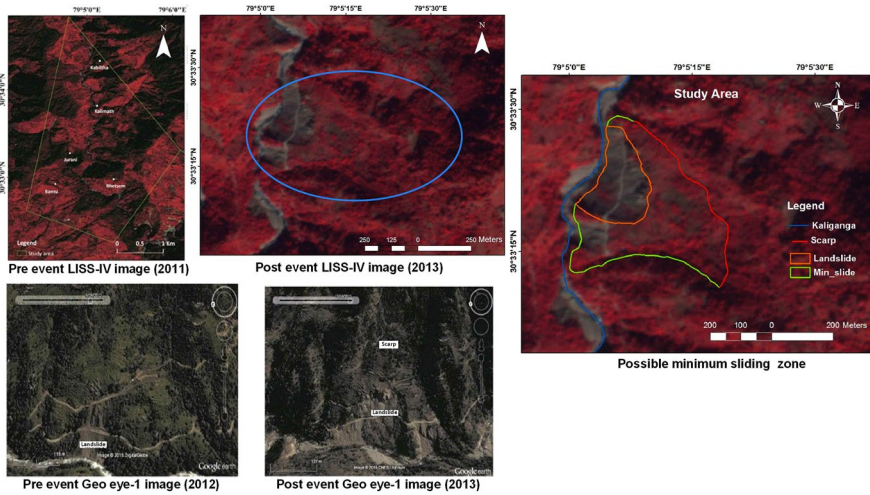


Fig. 3 Delineation of landslide zone based on satellite image interpretation, geophysical survey and field investigation

Chattoraj and Champati ray 2015; Chattoraj 2017; Dobhal et al. 2013). Therefore, to assess the triggering potential based on threshold equation developed for similar regions in the Garhwal Himalaya, precipitation data of 2012, 2013, 2014 and 2015 were extracted from the TRMM (Tropical Rainfall Measuring Mission) 3B42 V.7. The rainfall intensity data at daily interval from 1st January 2012 to 31st October 2015 have been downloaded in netCDF format and then converted to tiff by using multi-dimension toolbox in Arc-GIS software for further evaluation. The duration is calculated from the ‘daily files’ which are stacked to generate a ‘monthly file,’ and from the monthly stack, the duration is presented as ‘the days of continuous rainfall’. To calculate the minimum precipitation threshold, a relationship between the landslide event, 3-day cumulative rainfall data and previous 15 days antecedent rainfall data has been established for the Alaknanda River catchment in the Uttarakhand Himalaya by Kuthari (2007). This relationship is dependent on the geology, geomorphology, land use and climate of the area. The same model was used to derive T_6 threshold given as:

$$T_6 = R_3 + 1.5351R_{15} - 179,$$

where T_6 is the minimum threshold correlated with at least six landslides along the highway in the study area; R_3 is the 3-day cumulative rainfall measurement; and R_{15} is the 15-day antecedent rainfall measurement prior to the 3-day precipitation. To evaluate the main triggering factor for scarp formation and landslide initiation, plots of T_6 and daily precipitation values for 2012 to 2015 were generated.

4.2 Satellite image analysis

Using high-resolution satellite images of IRS LISS-IV for both pre-event (2011) and post-event (2013), Kunjethi landslide and associated scarp were detected. Left bank of the Kalganga river revealed a spectacular curvilinear scarp on satellite image of 2013 (Fig. 3). This was apparent on the image due to tonal contrast. To assess the temporal changes

associated with the scarp formation satellite images available in Google Earth (Quick Bird satellite images) were also referred (Fig. 3). The scarp extends from Kunjethi village and culminates at a major lineament present on the southern side of it (Fig. 3). By using temporal (2011–2013) satellite images (LISS-IV) and field observations, it was easy to zero-in locations and areal extent of the scarp and active landside zone, which later on was analysed by geophysical means.

4.3 Geophysical investigations

Both GPR and ERT methods are capable of producing high-resolution images. It should be noted that they depict different physical properties of the strata in terms of different dielectric constants in GPR and resistivity in ERT techniques. ERT methods are based on the variation of electrical resistivity of the subsurface material. The method is based on single-channel 4-electrode arrays, where 2 are used for current injection and 2 for voltage measurements. The surveys were carried out by a Lippmann 4 point light 10 W IP earth resistivity meter, coupled with a multi-electrode system (40 electrodes), using pole–dipole and dipole–dipole configurations to obtain different investigation depth. An electronic switching unit automatically selects the four electrodes needed for each measurement. Data acquisition was done using Geotest software (© Dr. Rauen) with an electrode spacing of 2.5 m and 5 m for an array length of 100 and 200 m, respectively.

Binley and Kemna (2005) stressed upon that ‘inverse problem’ needs to be solved. This means a given a set of measurements (data), the distribution of electrical properties (model) is sought to check the degree of acceptability of observations. In case of resistivity surveys, data will be in the form of transfer resistances or apparent resistivities, while in case of IP survey, it will be in the form of apparent chargeability or transfer impedance. The models will be parameterized in terms of resistivity or conductivity and intrinsic chargeability or complex resistivity, respectively.

Loke and Barker (1996), Binley and Kemna (2005) found no unique solution to this problem and agreed that an infinite number of models, in principal, should fit the data within a known level of uncertainty. They suggested a solution by formulating the inverse problem as a regularized optimization problem, which involves minimization of an objective function comprising both data misfit (measured vs. modelled). Similar approach has been adopted in our study, and it is observed that there is subtle difference in measured pseudo resistivity section versus modelled (forward) resistivity section. This proves the fidelity of the methodology adopted. Consequently, finite element (FE) or finite difference (FD) methods have unanimously been used for these problems.

The 2-D section along profile A–B, C–D, and E–F (Fig. 4) were obtained by pole–dipole configuration with 40 electrodes. Profile length of A–B was 100 m while that of C–D and E–F was 200 m. Separation between electrodes in case of A–B was 2.5 m, and for rest two it was 5 m. Tomography section along A–B was taken near to scarp/head of the slide, slightly cutting across the scarp, while C–D and E–F profiles were taken within the body of the landslide in the middle part in such a way that these cover most part of the landslide to capture heterogeneity. Profile XY (dipole–dipole method) has been analysed in next section. Therefore, depth of investigation is higher in C–D and E–F profiles than A–B. The investigation depth of A–B was 38.6 m, while other two profiles were 77.2 m. The length along the slope in A–B was 100 m and others were 200 m. The RMS error of A–B, C–D and E–F are 7.1, 6.1 and 7.2, respectively. The resistivity values of each profile range from 83 to 48118 Ω -m. The pole–dipole

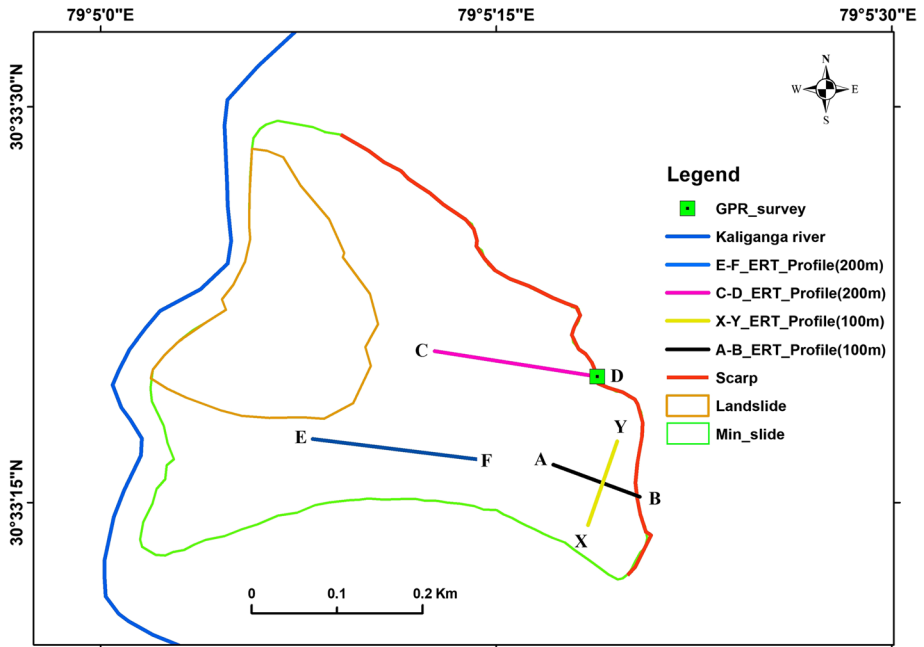


Fig. 4 Locations of geophysical surveys

configuration provided good lateral resistivity contrast and higher depth of investigation compared to other configurations. As the terrain is rugged with unidirectional varying slope gradient, topographic corrections were applied by providing actual elevation information of the electrodes during modelling/inversion. The X–Y section was taken along (Fig. 4) with dipole–dipole configuration of 40 electrodes at an interval of 2.5 m and length of 100 m. The pole–dipole configuration was not implemented along the scarp because of space constraints. Although dipole–dipole configuration had a shallower depth of investigation compared to the pole–dipole configuration, it provides good horizontal coverage (Fig. 5).

Ground penetrating radar (GPR) is a proven technique capable of providing highest possible resolution (using 100 MHz antennae) suitable for shallow subsurface exploration (Asprion et al. 1997; Reicherter and Reiss 2001a, b; Bristow and Jol 2003; Reiss et al. 2003). The GPR profiles were obtained with 100 MHz shielded antennas and GRED HD viewer software. A transmitter antenna radiates very short pulses into the subsurface. From boundaries with dielectric contrasts, the pulses are reflected back to a receiver antenna at the surface. A series of scans are collected as the antenna, moved along a survey line, typically in constant offset method. These scans form a display profile of the subsurface when positioned side by side and combined with marks indicating the current position of the antenna. After testing multiple options, the following processing scheme was selected: (1) move start time: automatic; (2) Dewow filtering: automatically applied; (3) time domain band-pass filtering: 50–100 MHz for 100 MHz antenna; and (4) background removal: to a maximum depth of 5 m for the 100 MHz. Time–depth conversion was done by GRED HD software (© Georeva).

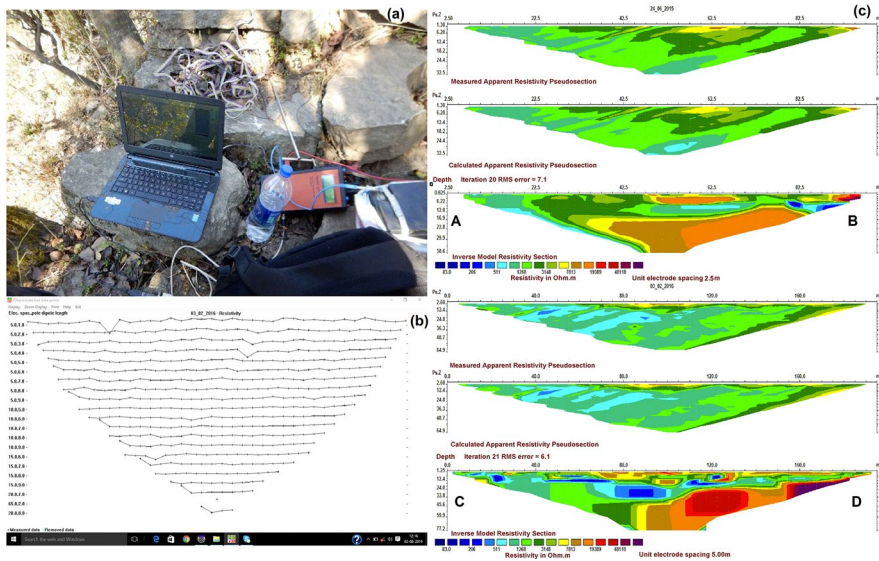


Fig. 5 **a** Resistivity data acquisition, **b** exterminate some bad data points, **c** depth sections showing the process to derive the calculation of true resistivity through measured and calculated (through forward modeling) apparent resistivity data of subsurface, parallel to the longitudinal axis of the possible landslide (A–B and C–D profile lines)

5 Results and discussion

5.1 Precipitation analysis

In order to evaluate the main triggering factor for scarp formation and landslide initiation, precipitation data of 2012, 2013, 2014 and 2015 were extracted from TRMM 3B42 V.7 data sets and precipitation threshold equation developed for similar regions in the Garhwal Himalaya was applied (Mathew et al. 2013). This equation takes into account the previous 3-day precipitation (including the day in consideration) and 15-day prior cumulative precipitation to account for antecedent moisture condition. It was observed that the threshold value is very high during summer monsoon months July to September particularly in the year 2013, when it had crossed 600 compared to around 200 in 2015 (Fig. 6). In the year 2013, extreme precipitation during first half of June resulted in unprecedented rise in threshold value on June 16th 2013 which ultimately led to the formation of scarp and initiation of landslide because of high saturation of soil. Local population also verified the same information during field investigation. There could have been some amount of slope movement in 2012 and 2014, but it could not be confirmed as the area is under cultivation (subtle evidences are obliterated) and local population could not confirm it (Fig. 7).

5.2 Geophysical data analysis

By using the two geophysical methods, ERT and GPR, the data were collected along five profiles (Figs. 8, 9). GPR survey was carried out at one location close to northern boundary

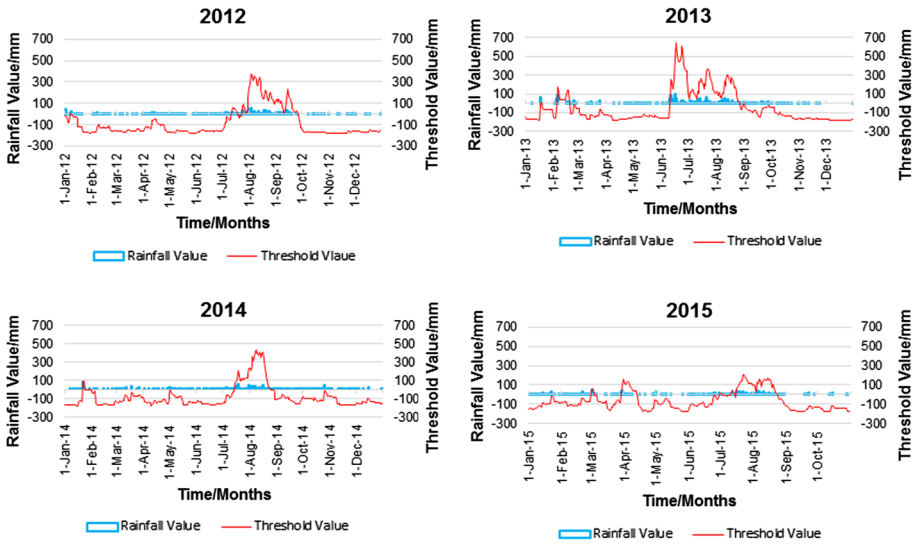


Fig. 6 Rainfall and threshold plot for 2012, 2013, 2014 and 2015 reveals extreme precipitation event of 2013, which acted as triggering factor for landslide at Kunjethi (Kalimath)



Fig. 7 **a** Developed scarp during 2013 extreme rainfall event of Kedarnath disaster, **b** tension cracks appeared on the unstable landmass, **c** damaged house which is located very close to crown of the landslide, **d** spring water along the flow path

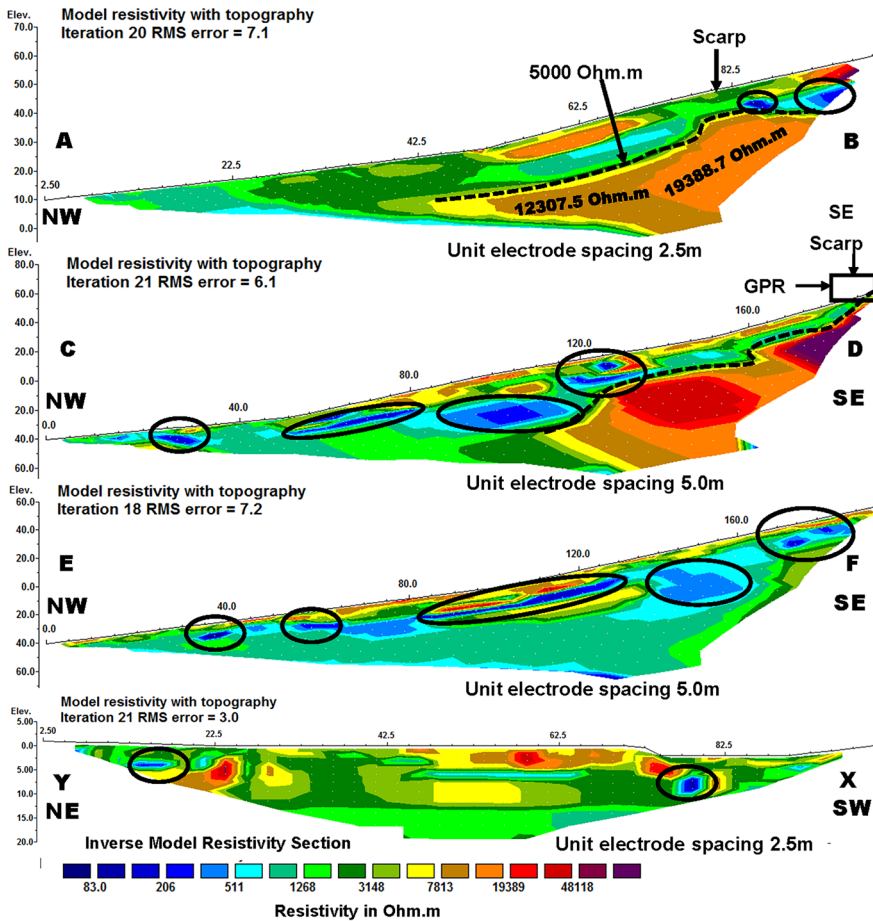


Fig. 8 Depth section showing true resistivity values of subsurface parallel to the longitudinal axis of the possible landslide (A–B, C–D and E–F sections) and transverse to the slide (X–Y section), derived through pole–dipole configuration (A–B, C–D and E–F sections) and dipole–dipole configuration (X–Y section) with topographic correction. The dotted line shows the possible slip surface. The high water saturation are marked by black coloured circles

of scarp, while ERT survey was carried out along four transects mostly within the landslide body/mass and across the scarp (Fig. 4).

5.2.1 Two-dimensional ERT survey along profile: A–B, C–D and E–F

Figure 8 shows inverted profiles with topographic correction of three profiles, which were obtained in a direction parallel to the longitudinal axis of the landslide. The most striking feature of A–B and C–D profiles is the sharp lateral discontinuities across which the resistivity values changes drastically in vertical direction. The sharp discontinuity in Fig. 8 is interpreted as the possible slip surface or failure plane that separates the landslide overburden mass/slide materials from the stable bedrock/underlying mass.

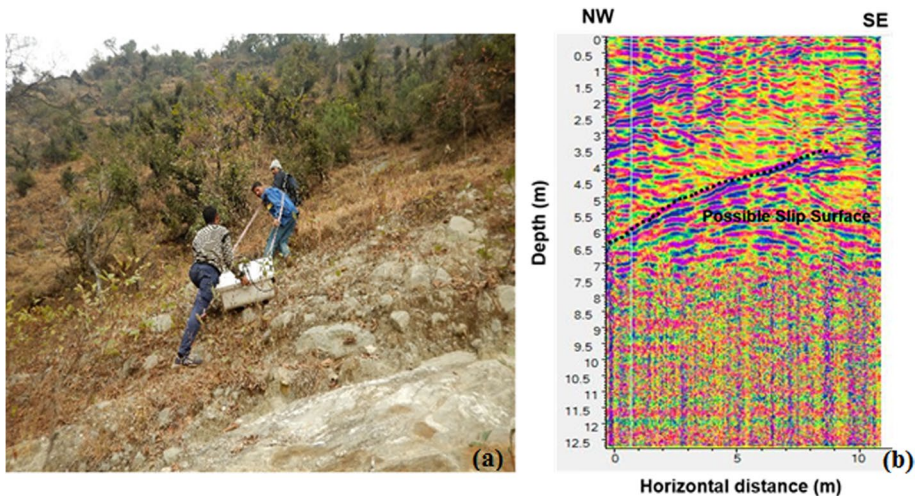


Fig. 9 **a** GPR data acquisition across the scarp, **b** GPR profile radargram very close to scarp in C–D profile (Fig. 4)

Directly beneath the slip surface, a sharp rise in the resistivity values from approximately 5000–19,000 Ω -m was observed which is interpreted as a detrital mass of basement rock. Based on the literature (Telford et al. 1990) and field observation, basement rock is related to granite gneiss/augen gneiss. The recently developed scarp is at approximately between 82.5 m and 190 m from the profile origin node at A and C, respectively. A sharp decrease in the resistivity value is noted just below the scar in the A–B tomography section. The C–D profile shows depth of the bedrock to increase in a step-like fashion (down-slope) which is clearly a resultant of sliding.

Using A–B and C–D resistivity profiles, weighted average depth to slip surface in each profile has been estimated separately. Calculated weighted average depth to slip surface in A–B and C–D profiles are 15 m and 19 m, respectively. As explained above, A–B section was taken close to head-ward portion of the landslide while C–D section was towards middle of the landslide. Slip surface is usually concave upward and maximum depth was obtained in middle portion as a result the depth to slip surface is higher in C–D profile.

These profiles reveal that thickness of the overburden material is relatively thin compared to deep-seated landslides, and as a result it requires less amount of water for saturation leading to landslide. The depth to bedrock becomes shallower towards the landslide scarp, where incidentally saturation is also high. In the upslope direction of A–B profile, a zone of very high conductivity succeeds the landslide scarp expression, which could allow water seepage leading to landslide.

Another prominent feature of these sections (A–B, C–D and E–F) is anomalously high-resistivity zones at almost near-surface level, which could be interpreted as former landslide debris. This is supported by the field evidence of presence of weathered derivatives of mainly gneissic and schistose rocks and other meta-sedimentary rocks on a sloping terrain. The sections along C–D and E–F show presence of high saturated zones which could cause decrease in soil strength and facilitate movement of the landslide. This was also confirmed by field evidences of tension cracks and subsidence in different parts of the landslide body.

5.2.2 Interpretation along ERT profile X–Y

This profile is almost perpendicular to A–B profile and does not cut through the landslide scarp. It was located just below the scarp and runs parallel to it. In this case, the depth of investigation was reached up to 19.7 m with an RMS error of 3.0.

A zone of high resistivity, more than 5000 Ω -m, is present at shallow surface, which could be correlated with the anomalous high resistive body present in profile A–B. The underlying low resistivity lens is also in agreement with the presence of similar material in sections A–B. As the total depth of investigation is less in dipole–dipole configuration, slip surface could not be mapped. Overall, this section with dipole–dipole configuration brings out the presence of a highly resistive body which correlates well with the A–B profile obtained with pole–dipole configuration. It also confirms the localized nature of the high-resistivity mass, which is interpreted as detrital mass (Fig. 10).

5.3 Ground penetrating radar profile

GPR profile was acquired with 100 MHz antenna across the developed scarp along the south-eastern end of C–D profile (Fig. 4). This profile was acquired from NW to SE direction and the maximum depth of penetration reached up to 6.5 m. Steeply dipping reflector was clearly identified in GPR radargram corresponding to the slip surface identified in the ERT profile (Figs. 8, 9). Significant amount of radar reflection was observed along this boundary mainly due to the change in dielectric properties of the underlying materials across the slip surface. Although GPR technique was found capable to provide crucial

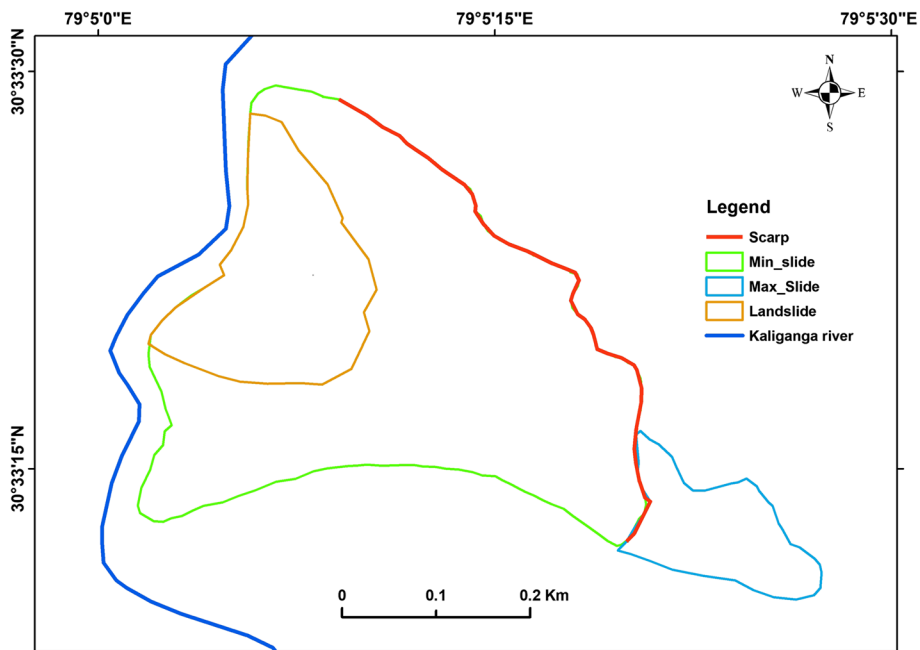


Fig. 10 Active landslide zone, scarp and possible extensions as detected by satellite imagery and geophysical survey

information at one location, highly rugged topography inhibited its application in other areas of scarp. Compared to ERT, the depth of penetration was less in case of GPR which was one of the limitations in this rugged mountaineous terrain. The NW part of radargram shows uneven reflection mainly from the landslide debris, which was confirmed by presence of angular to sub-angular boulders during field investigation. At this particular location, depth to the possible slip surface is estimated at 6 m from ERT survey and at 6.5 m from GPR profile. Approximately same depth of the slip surface was confirmed by both the geophysical techniques, which have provided very useful complimentary and confirmatory evidences.

5.4 Mapping of possible maximum sliding zone

Based on the location of landslide (2013) scarp, landslide prior to 2013, physical boundary of southern side and field observations, landslide zone was demarcated (Fig. 3). As per the resistivity profile obtained along C–D, slip surface has not extended above the scarp, and during the field investigation, rock outcrops of bedrock was observed above the scarp (towards upper slope). So northern boundary of the possible sliding mass extends up to the observed scarp. In resistivity profile of A–B, obtained across the scarp (Fig. 4), some loose unconsolidated material was observed in the up slope direction, affected by gully erosion and minor slope failures. Therefore, based on the geophysical investigation, analysis of satellite image and field observations, the maximum extent of landslide has been mapped. Additionally, the approximate volume estimated for the active landslide portion comes to be about 32,300 cubic metre, as estimated from field measurement and satellite data analysis (considering manually field measured avg. depth of 80 cm of soil).

6 Landslide remedial measures

The results of the study are of utmost importance to disaster management primarily due to three reasons: (1) the entire disturbed mass can slide down, block the river and cause inundation in upstream and possibility of breaching of landslide dam and flooding in the downstream; (2) there are human population living on the disturbed mass, who need to be informed about the progress and possibility of such a catastrophic event; and (3) such studies are essential at many such locations where fractures and scarps have developed, and it is very essential to know the possible slip surface/failure plane before designing any remedial measures.

In the event of entire landslide mass sliding and blocking the Kaliganga River, it can lead to a major disaster in the Kaliganga and Mandakini and subsequently in Alaknanda valley. The valley of Madhyamaheswar Ganga, across the mountain range to the east, had experienced catastrophic landslide and blockade of river in 1998 and even prior to this as revealed by satellite image analysis (Sah and Bisht 1998).

Therefore, as the area is prone to large landslides and river blockades, every attempt should be made to avoid such an event. Towards this, it is recommended to maintain the stability of the disturbed mass at Kunjethi village by making at least three preventive measures such as maintaining flow of the existing channel particularly towards southern boundary of the landslide mass along a prominent lineament. If need arises, proper lining and steps for cascading should be constructed to maintain maximum flow and reduce bank erosion. Secondly, attempt must be made to dewater the landslide mass by providing adequate

drainage measures. Since the area is under cultivation, it is important to make an assessment of the irrigation water requirement and drainage provisions. Any amount of excess water should be allowed to flow down the landslide mass through lined channel. Thirdly, as a monitoring mechanism, at couple of locations piezometers must be installed up to a depth of 15 metres to assess the rising in water table and subsequent movement of landslide mass by repeat GPS observations. Lastly, attempt must be made to contain the bank erosion at the toe of the landslide mass by making suitable remedial measures. Such basic remedial measures and monitoring mechanism will go a long way to prevent the catastrophic effect of the landslide and minimize the risk to life and property.

7 Conclusions

Landslides, the most widespread hazards in the Himalayan terrain, result in huge loss of life and property every year. The main emphasis of the paper was on early detection of landslide by analysing remotely sensed satellite data products and geophysical investigations (ERT and GPR) for subsurface characterization and detection of slip surface. During routine survey by using satellite remote sensing, a curvilinear scarp was detected which was confirmed to be associated with slow moving landslide and it was initiated during extreme high precipitation June 2013, as evidenced by rainfall threshold analysis and field observation. The geophysical survey such as ERT and GPR has enabled subsurface characterization and helped to identify the slip surface which shows good correlation with the weak zone where the landslide scarp has been formed. Four ERT profiles were used to determine the approximate depth to slip surface, which is estimated to be around 15 m to 19 m. One high-resolution GPR radargram profile obtained very close to scarp confirmed the depth of slip surface as observed in the ERT profile. The geophysical investigations, field observation and sample analysis have confirmed the presence of moisture zones/clay enrich wet debris within the overburden, which is inferred as main contributing factor for landslide initiation. Integration of satellite remote sensing, geophysical studies and field observations has been used to delineate and map the maximum possible sliding zone. Overall, the Kunjethi landslide is unique as it represents a smaller landslide due to toe cutting within a body of larger destabilized mass marked by the recent scarp development on relatively gentle sloping landmass underlain by colluvial deposits of metamorphic rocks (mainly gneissic and schistose rocks). Therefore, attempt must be made to take remedial measures for both the landslides separately as discussed. Towards this, identification of slip surface is crucial, and geophysical techniques have provided such information which is routinely required for designing mitigation measures in many vulnerable slopes.

Acknowledgements Facilities provided at Indian Institute of Remote Sensing, ISRO, Dehradun, are gratefully acknowledged. Study was supported under Disaster Management Support Programme of ISRO. Special thanks to Director, IIRS, for constant encouragement and support.

References

- Asprion U, Reicherter K, Meschede M (1997) The ground penetrating radar and its application for the detection of tectonic structures: an example from the Freudenstädter Graben (Black Forest southwest Germany). Annual reports and communications of the Upper Rhine geological Association New Series, vol 79, pp 111–124

- Bhattacharjee S, Champati Ray PK, Chatteraj SL, Dhara M (2017) Precipitation intensity-duration based threshold analysis for initiation of landslides in upper Alaknanda Valley. *Int J Environ Chem Ecol Geol Geophys Eng* 11(2):105–109
- Bichler A, Bobrowsky P, Best M, Douma M, Hunter J, Calvert T, Burns R (2004) Three-dimensional mapping of a landslide using a multi-geophysical approach: the Quesnel Forks landslide. *Landslides* 1:29–40
- Binley A, Kemna A (2005) DC resistivity and induced polarization methods. In: Yuram R, Hubbard S (eds) *Hydrogeophysics*. Water and Science Technology Library 50. Springer, New York, pp 129–156
- Bist KS, Sinha AK (1980) Some observations on the geological and structural setup of Okhimath area in Garhwal Himalaya; a preliminary report. *Himalayan Geol* 10:467–475
- Bogoslovsky VA, Ogilvy AA (1977) Geophysical methods for the investigation of landslides. *Geophysics* 42:562–571
- Bristow CS, Jol HM (2003) Ground penetrating radar: applications in sediments. *Geol Soc Lond Spec Publ* 211:338
- Castellanos Abella EA, Van Westen CJ (2008) Qualitative landslide susceptibility assessment by multicriteria analysis: a case study from San Antonio del Sur Guantánamo Cuba. *Geomorphology* 94:453–466
- Champati ray PK, Chatteraj SL, Chand DS, Kannaujiya S (2013) Aftermath of Uttarakhand disaster 2013: an appraisal on risk assessment and remedial measures for Yamunotri shrine using satellite image interpretation. *Indian Landslides* 6(2):61–70
- Champati ray PK, Chatteraj SL, Kannaujiya S, Bisht MPS, Pandey K, Goswami A (2015) Kedarnath disaster 2013: causes and consequences using remote sensing inputs. *Nat Hazards* 81(1):227–243. <https://doi.org/10.1007/s11069-015-2076-0>
- Chatteraj SL (2017) Debris flow modelling and risk assessment of selected landslides from Uttarakhand-case studies using earth observation data. In: Santra A, Santra S (eds) *Remote sensing techniques and GIS applications in earth and environmental studies (chapter-6)*. IGI Publications, Hershey, pp 111–121
- Chatteraj SL, Champati ray PK (2015) Simulation and modelling of debris flows using satellite derived data: a case study from Kedarnath area. *Int J Geomat Geosci* 6(2):1498–1511
- Chatteraj SL, Champati Ray PK, Kannaujiya S (2017) Simulation outputs of major debris flows in Garhwal Himalaya: a geotechnical modelling approach for hazard mitigation. In: Navalgund RR, Senthil Kumar A, Nandy S (eds) *Remote sensing of northwest himalayan ecosystems*. Springer, New Delhi. <https://doi.org/10.4018/978-1-5225-1814-3.ch006>
- Cruden DM (1991) A simple definition of a landslide *Bulletin International Association for. Eng Geol* 43:27–29
- Dobhal DP, Gupta AK, Metha M, Khandelwal DD (2013) Kedarnath disaster: facts and plausible causes. *Curr Sci* 105(2):171–174
- Friedel S, Thielen A, Springman SM (2006) Investigation of a slope endangered by rainfall-induced landslides using 3D resistivity tomography and geotechnical testing. *J Appl Geophys* 60(2):100–114
- Godio A, Strobbia C, De Bacco G (2006) Geophysical characterisation of a rockslide in an alpine region. *Eng Geol* 83:273–286
- Hack R (2000) Geophysics for slope stability. *Surv Geophys* 21:423–448
- Hunt RE (1984) *Geotechnical engineering investigation manual*. McGraw-Hill, New York, pp 665–784
- Jongmans D, Garambois S (2007) Geophysical investigation 500 of landslides: a review. *Bulletin de la Société géologique de France* 178(2):101–112
- Kuthari S (2007) Establishing precipitation thresholds for landslide initiation along with slope characterisation using GIS-based modeling. M.Sc. dissertation ITC Enschede, The Netherlands
- Lapenna J, Lorenzo P, Perrone A, Piscitelli S, Rizzo E, Sdao F (2005) 2D electrical resistivity imaging of some complex landslides in Lucanian Apennine chain southern Italy. *Geophysics* 70(3):B11–B18
- Loke MH, Barker RD (1996) Rapid least-squares inversion of apparent resistivity pseudo sections using a quasi-Newton method. *Geophys Prospect* 44:131–152
- Mathew J, Babu G, Kundu S, Kumar VK, Pant CC (2013) Integrating intensity-duration based rainfall threshold and antecedent rainfall-based probability estimate towards generating early warning for rainfall-induced landslides in parts of Garhwal Himalaya, India. Springer, Berlin
- McGuffey V, Modeer J, Victor A, Turner AK (1996) *Subsurface exploration in landslides: investigation and mitigation*. Special Report National Academy Press Washington DC, pp 231–277
- Meric O, Garambois S, Jongmans D, Wathelet M, Chatelain J, Vengeon J (2005) Application of geophysical methods for the investigation of the large gravitational mass movement of sechillienne france. *Can Geotech J* 42:1105–1115

- Perrone A, Zeni G, Piscitelli S, Pepe A, Loperte A, Lapenna V, Lanari R (2006) Joint analysis of SAR interferometry and electrical resistivity tomography surveys for investigating ground deformation: the case-study of Satriano di Lucania (Potenza Italy). *Eng Geol* 88:260–273
- Petley DN (2012) Global patterns of loss of life from landslides. *Geology* 40(10):927–930
- Reicherter K, Reiss S (2001a) The Carboneras Fault Zone (southeastern Spain) revisited with Ground Penetrating Radar—Quaternary structural styles from high-resolution images. *Geology en Mijnbow Netherlands J Earth Sci* 80:11–20
- Reicherter K, Reiss S (2001b) Active faults in the Cubillas reservoir area mapped by 3D ground penetrating radar imaging (northeastern Granada Basin southern Spain) *Zentralblatt. Geol Paleontol* 1:167–179
- Reiss S, Reicherter K, Reuther CD (2003) Visualization and characterization of active normal faults and associated sedimentary structures by high-resolution ground penetrating radar (GPR) In: Bristow CS, Jol HM (eds) *Ground penetrating radar in sediments*, vol 211. Geological Society London Special Publication, pp 247–255
- Sah MP, Bisht KS (1998) Catastrophic mass movement of August 1998 in Okhimath area Garhwal Himalaya In: *Proceeding of international workshop cum training programme on landslide hazard and risk assessment and damage control for sustainable development New Delhi*, pp 259–282
- Sass O, Bell R, Glade T (2008) Comparison of GPR 2D-resistivity and traditional techniques for the subsurface exploration of the Öschingen landslide Swabian Alb (Germany). *Geomorphology* 93(1–2):89–103
- Telford WM, Geldart LP, Sheriff RE (1990) *Applied geophysics*. Cambridge University Press, Cambridge, p 770
- Valdiya KS, Paul SK, Chandra T, Bhakuni SS, Upadhyay RC (1999) Tectonic and lithological characterization of Himadri (Great Himalaya) between Kali and Yamuna rivers central Himalaya. *Himal Geol* 20:1–17

Publisher's Note Springer Nature remains neutral with regard to jurisdictional claims in published maps and institutional affiliations.